bioRxiv preprint doi: https://doi.org/10.64898/2026.06.26.734747; this version posted August 4, 2026. The copyright holder for this preprint (which was not certified by peer review) is the author/funder, who has granted bioRxiv a license to display the preprint in perpetuity. It is made available under a CC-BY-NC-ND 4.0 International license.

Modular split-trigger cooperative activation enables a programmable Cas13-12 cascade

Rui Sang [1], Ewa M. Goldys [1, *], Fei Deng [1, *]

[1]School of Biomedical Engineering, Faculty of Engineering, University of New South Wales, Sydney, NSW 2052, Australia

* Correspondence: e.goldys@unsw.edu.au; fei.deng@unsw.edu.au;

Abstract

Achieving precise control of CRISPR/Cas *trans*-cleavage depends on understanding how nucleic acid activators engage Cas effectors, yet the fundamental principles of split-trigger activation of Cas12a remain unclear. Here, we uncover the mechanistic determinants that enable fragmented nucleic acids to collectively initiate Cas12a activity. We show that split triggers bearing external extensions fully support the R-loop formation, whereas internal extensions which disrupt the spacer complementarity abolish Csa12a activation. We further demonstrate that covalent linkage of split-trigger fragments prevents R-loop propagation, revealing that Cas12a's activation strictly requires two physically independent split fragments. Together, these findings establish a synergistic split-trigger activation mechanism in which cooperative hybridization of two individually fragments nucleates and extends the Cas12a R-loop with high efficiency. Conceptually, this mechanism enables a cascade architecture that transforms CRISPR diagnostics from a one-target one-Cas ribonucleoprotein (RNP) paradigm into a highly amplifying process in which a single target molecule activates numerous downstream Cas RNPs. Building on this principle, we show that the cleavage of a rationally designed linear DNA-RNA-DNA mediator by LbuCas13a generates optimally configured split triggers for Cas12a activation, thereby coupling RNA recognition to large-scale Cas12a activation without enzymatic

bioRxiv preprint doi: https://doi.org/10.64898/2026.06.26.734747; this version posted August 4, 2026. The copyright holder for this preprint (which was not certified by peer review) is the author/funder, who has granted bioRxiv a license to display the preprint in perpetuity. It is made available under a CC-BY-NC-ND 4.0 International license.

preamplification. The resulting Split Trigger Activated Cas13-Cas12 Cascade System (STACS) achieves amplification-free detection down to 1 copy/μL within 15 minutes and maintains robust performance in complex biological (serum, saliva) and environmental (mud) matrices. This work establishes a generalizable strategy for engineering programmable CRISPR cascades with high Cas RNP activation multiplicity for ultrasensitive molecular diagnostics.

Keywords

Split-trigger, CRISPR cascade amplification, amplification-free RNA detection, Cas13-12 tandem system

Introduction

Precise control of CRISPR/Cas *trans*-cleavage requires a detailed understanding of how nucleic acid activators engage Cas effectors (1). In CRISPR-based sensing, target recognition by a guide RNA initiates R-loop formation between the crRNA spacer and the complementary nucleic acid sequence, which the induces indiscriminate *trans*-cleavage activity of the Cas nuclease against single-stranded nucleic acid reporters (2-4). This target triggered signal amplification mechanism has extended the applications of CRISPR/Cas systems beyond gene editing enabling versatile molecular sensing and it underpins the sensitivity and specificity of CRISPR diagnostics (5). Consequently, the molecular rules governing Cas activation - rather than the downstream signal readout alone - represent a fundamental constraint in CRISPR-based nucleic acid detection.

Extensive efforts have been devoted to engineering nucleic acid activators to modulate Cas12a activity (6). Variations in activator length, nucleotide composition, and structural topology - including elongated activators, random 3′ extensions, dangling-end stabilization, DNA-RNA

bioRxiv preprint doi: https://doi.org/10.64898/2026.06.26.734747; this version posted August 4, 2026. The copyright holder for this preprint (which was not certified by peer review) is the author/funder, who has granted bioRxiv a license to display the preprint in perpetuity. It is made available under a CC-BY-NC-ND 4.0 International license.

chimeric triggers, and sterically constrained architectures, have revealed that Cas12a activation is highly sensitive to trigger geometry and flexibility (7-11). These studies have significantly advanced the understanding of R-loop formation and *trans*-cleavage kinetics. However, the mechanistic insights obtained thus far are almost exclusively derived from contiguous activators. As a result, current design rules remain confined to single-molecule trigger paradigms and do not address whether smaller fragments of such triggers, each with suboptimal length can reliably initiate and sustain Cas12a activation by synergistic action.

Recent studies provide initial evidence that split activators can modulate Cas12a activity under certain conditions. PAM-proximal helper strands have been shown to rescue Cas12a activation by replacing the DNA spacer region with RNA targets, enabling amplification-free detection of viral RNA and microRNAs (12). In parallel, cooperative activation has been observed when two short ssDNA fragments are simultaneously present, leading to enhanced *trans*-cleavage and improved mismatch discrimination (13). Mechanistic models such as induced targeting and exon-unwinding have been proposed to interpret these phenomena (14). Nevertheless, these reports primarily describe phenomenological activation behavior and do not establish generalizable molecular rules governing fragment orientation, extension position, physical linkage, or R-loop propagation. As a result, the principles by which split triggers nucleate and extend the Cas12a R-loop remain undefined.

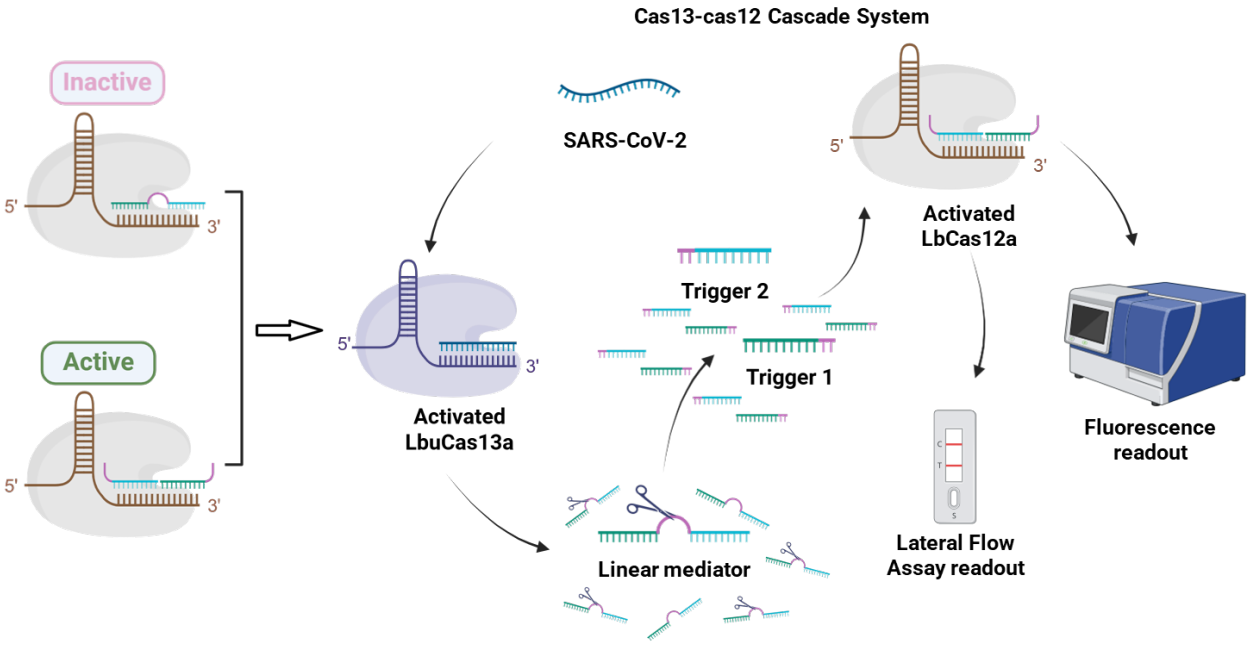
Here, we systematically define the molecular rules governing Cas12a activation by split nucleic acid triggers. We demonstrate that split triggers bearing external nucleotide extensions fully support R-loop formation, whereas internal extensions disrupt spacer complementarity and abolish activation. We further establish that Cas12a activation strictly requires two physically independent fragments, as covalent linkage prevents productive R-loop propagation. By

bioRxiv preprint doi: https://doi.org/10.64898/2026.06.26.734747; this version posted August 4, 2026. The copyright holder for this preprint (which was not certified by peer review) is the author/funder, who has granted bioRxiv a license to display the preprint in perpetuity. It is made available under a CC-BY-NC-ND 4.0 International license.

systematically mapping fragment length effects, we reveal a division of labour in which one fragment nucleates R-loop initiation while the complementary fragment promotes R-loop extension and stabilization. Together, these findings establish a mechanistic framework for cooperative split-trigger mediated Cas12a activation.

Furthermore, we show that, as a direct consequence of these mechanistic constraints, the cleavage of a specially designed linear DNA-RNA-DNA mediator by LbuCas13a generates split fragments that are optimally configured for Cas12a activation. Leveraging this effect, we construct a Split Trigger Activated Cas13-Cas12 Cascade System (STACS), which transforms RNA recognition into sequential CRISPR amplification without enzymatic preamplification. Unlike conventional amplification-assisted CRISPR diagnostics(12,15), STACS achieves amplification-free detection down to 1 copy μL^{-1} of SARS-CoV-2 RNA within 15 minutes, with robust performance across complex biological and environmental matrices, including serum, saliva, and mud. Importantly, the linear mediator is prepared using standard commercial methods and is readily obtainable from many suppliers. Conceptually, this design transforms CRISPR diagnostics from a conventional one-target one-Cas ribonucleoprotein (RNP) paradigm into a cascade architecture in which a single target molecule triggers the activation of numerous downstream Cas RNPs. This work bridges fundamental CRISPR activation biology with practical diagnostic engineering and provides a mechanistic foundation for designing programmable CRISPR cascade systems.

bioRxiv preprint doi: https://doi.org/10.64898/2026.06.26.734747; this version posted August 4, 2026. The copyright holder for this preprint (which was not certified by peer review) is the author/funder, who has granted bioRxiv a license to display the preprint in perpetuity. It is made available under a CC-BY-NC-ND 4.0 International license.



Graphic abstract. Mechanism and detection workflow of the Split Trigger Activated Cas13-12 Cascade System (STACS).

Results

1. External-Extension split triggers efficiently activate LbCas12a

We first evaluated whether fragmented activators could support Cas12a *trans*-cleavage. The two pristine split fragments of a fully competent activator (trigger-1 and trigger-2) restored full activation when supplied together, yielding fluorescence kinetics equivalent to the intact activator, whereas either fragment alone showed minimal activity (Fig.1A and Fig. S1). These results confirm that Cas12a efficiently recognises a bipartite activator, provided that the complementary region required for R-loop formation remains intact.

bioRxiv preprint doi: https://doi.org/10.64898/2026.06.26.734747; this version posted August 4, 2026. The copyright holder for this preprint (which was not certified by peer review) is the author/funder, who has granted bioRxiv a license to display the preprint in perpetuity. It is made available under a CC-BY-NC-ND 4.0 International license.

To determine how nucleotide extensions influence this process, we compared split triggers carrying either external or internal poly-U additions. External extensions positioned at the 5′ end of trigger-1 or the 3′ end of trigger-2 preserved robust activation: individually inactive, the two extended fragments together triggered Cas12a with efficiency comparable to the intact activator (Fig.1B). In contrast, internal U-extensions inserted between the two complementary halves completely abolished activation, even when both fragments were supplied (Fig.1C). This loss of activity indicates that internal insertions obstruct productive pairing with the crRNA spacer and disrupt R-loop propagation.

Together, the structural schematics and kinetic data in Fig. 1 establish a clear mechanistic rule: Cas12a tolerates nucleotide extensions only when they lie outside the crRNA-target pairing region, whereas internal extensions disrupt R-loop formation and abolish activation. This positional requirement provides a straightforward design principle for constructing functional split triggers.

bioRxiv preprint doi: https://doi.org/10.64898/2026.06.26.734747; this version posted August 4, 2026. The copyright holder for this preprint (which was not certified by peer review) is the author/funder, who has granted bioRxiv a license to display the preprint in perpetuity. It is made available under a CC-BY-NC-ND 4.0 International license.

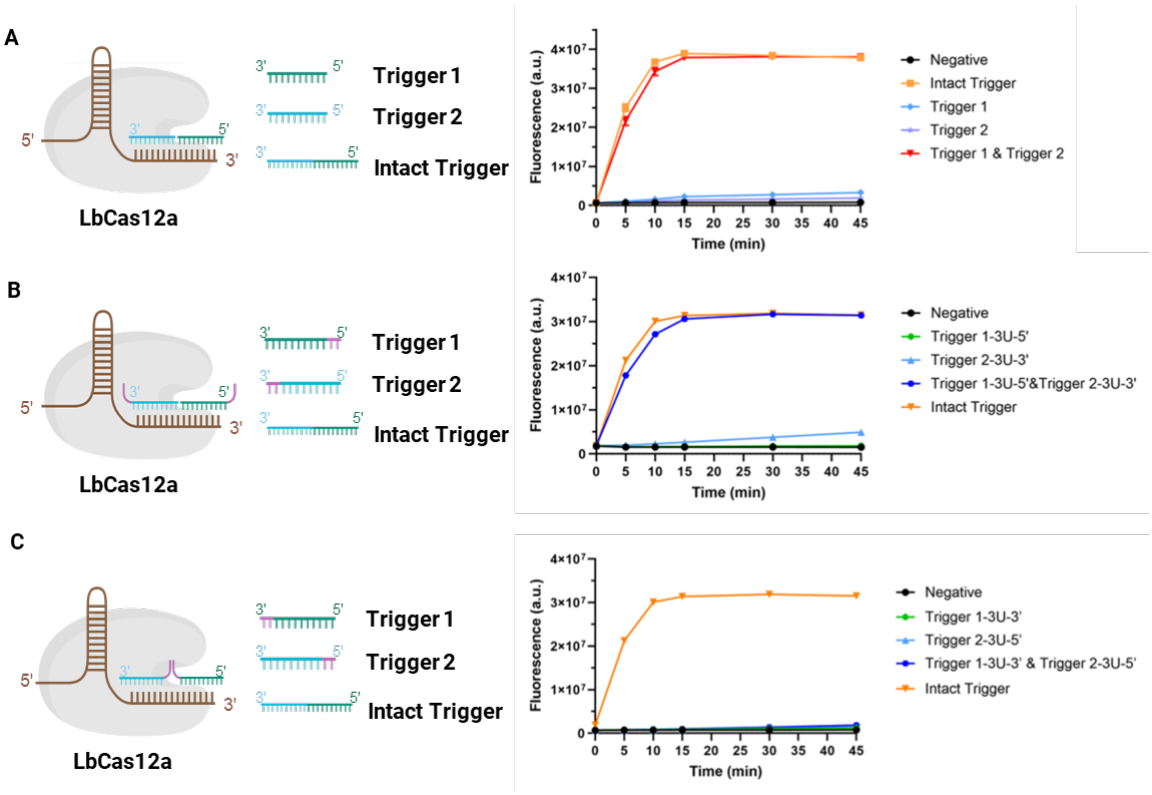


Figure 1. Split triggers with external extensions are able to fully activate LbCas12a. (A) Split triggers are able to fully activate LbCas12a; (B) Split triggers with external extensions are able to fully activate LbCas12a; (C) Split triggers with internal extensions are not able to activate LbCas12a. n=3, error bars represent mean ± SD, a.u = arbitrary units.

2. Linked split triggers fail to fully activate LbCas12a

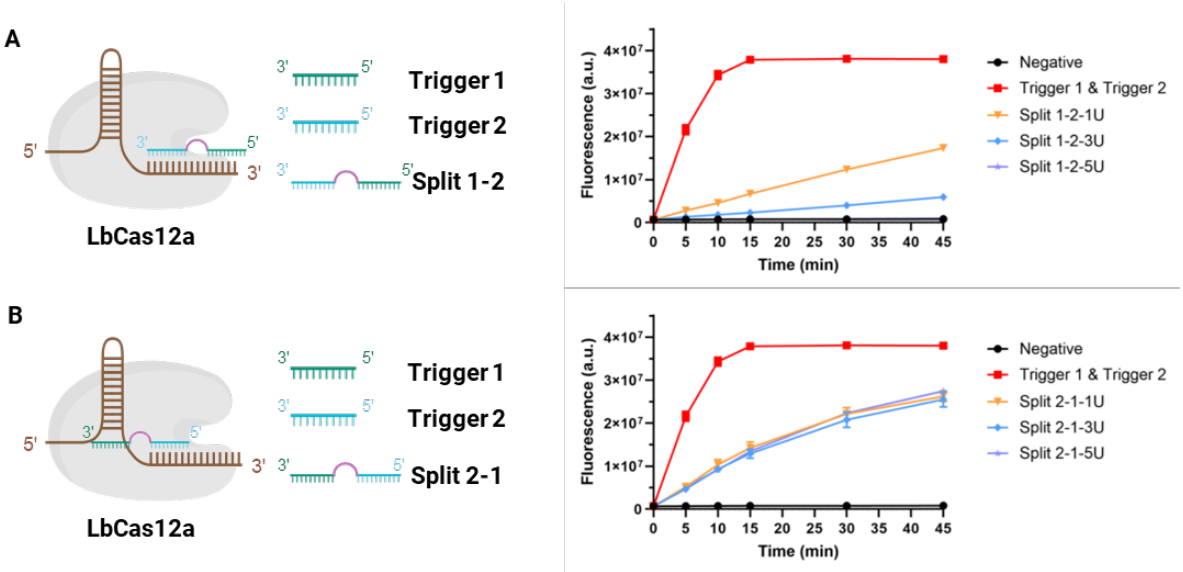
Having established that Cas12a tolerates *external* extensions on independent split fragments of trigger sequences, we next investigated whether these fragments could be covalently linked without compromising activation. To test this, we introduced poly-U linkers of varying lengths between trigger-1 and trigger-2 in two orientations (1→2 and 2→1), generating single-stranded constructs that retain full sequence complementarity but eliminate fragment independence (Fig. 2A-B).

bioRxiv preprint doi: https://doi.org/10.64898/2026.06.26.734747; this version posted August 4, 2026. The copyright holder for this preprint (which was not certified by peer review) is the author/funder, who has granted bioRxiv a license to display the preprint in perpetuity. It is made available under a CC-BY-NC-ND 4.0 International license.

Across all linker lengths examined, linked split triggers displayed markedly reduced activation compared with the unlinked trigger-1 + trigger-2 pair. When trigger-1 was positioned at the 5′ end (Split 1-2 constructs), increasing the U-linker length from 1-U to 5-U leads to lower activation efficiency, and none approached the activation level achieved by the two independent fragments (Fig. 2A). When the orientation was reversed (Split 2-1 constructs), all linked versions generated only partial activation despite increasing linker flexibility (Fig. 2B).

These results reveal a mechanistic constraint distinct from that observed for external extensions. Whereas Cas12a tolerates nucleotide additions outside the pairing region, it does not tolerate physical linkage between trigger fragments. We infer that covalent linkage restricts the conformational freedom required for sequential binding of the two halves and prevents the stepwise R-loop propagation observed with independent fragments.

Together, these findings establish that Cas12a activation requires two physically separate oligonucleotides, which bind the crRNA-guided complex in a coordinated but structurally unconstrained manner.



bioRxiv preprint doi: https://doi.org/10.64898/2026.06.26.734747; this version posted August 4, 2026. The copyright holder for this preprint (which was not certified by peer review) is the author/funder, who has granted bioRxiv a license to display the preprint in perpetuity. It is made available under a CC-BY-NC-ND 4.0 International license.

Figure 2. Linked split triggers are not able to fully activate LbCas12a. (A) The activation assessment of Split 1-2 with different U linker length for LbCas12a; (B) The activation assessment of Split 2-1 with different U linker length for LbCas12a. n=3, error bars represent mean ± SD, a.u = arbitrary units.

3. Defining the length requirements for functional split-trigger activation of LbCas12a

To define the length parameters governing efficient synergistic activation of LbCas12a, we systematically varied the lengths of trigger-1 and trigger-2 while maintaining their relative positions within the target sequence (Fig. 3A-H). For each trigger pair, Cas12a activation by the independent trigger-1 and trigger-2 fragments was compared with that produced by the corresponding linked split mediator, allowing direct assessment of synergy and background activation.

When trigger-1 was long (16-14 nt), trigger-1 alone was able to partially activate LbCas12a, and combining trigger-1 with trigger-2 resulted in only modest signal enhancement (Fig. 3B-D). In these configurations, the signal ratios between the paired triggers and the linked split mediators remained close to unity, indicating limited synergistic gain. This suggests that long trigger-1 fragments can independently nucleate R-loop formation, thereby reducing the relative contribution of cooperative activation.

As the length of trigger-1 was reduced to 13-12 nt, its standalone activation ability sharply decreased, and Cas12a activity became increasingly dependent on the presence of trigger-2 (Fig. 3E-F). Under these conditions, the paired trigger-1/trigger-2 combinations generated higher

bioRxiv preprint doi: https://doi.org/10.64898/2026.06.26.734747; this version posted August 4, 2026. The copyright holder for this preprint (which was not certified by peer review) is the author/funder, who has granted bioRxiv a license to display the preprint in perpetuity. It is made available under a CC-BY-NC-ND 4.0 International license.

signal ratios, consistent with a transition from single-fragment activation to cooperative R-loop assembly.

Maximal synergistic activation was observed when trigger-1 and trigger-2 were 11 nt and 10 nt in length, respectively (Fig. 3G). This configuration produced the highest fluorescence signal ratio (4.50), indicating optimal balance between insufficient standalone activation and efficient cooperative R-loop propagation. Further decrease of trigger-1 length to 10 nt reduced the signal ratio (Fig. 3H), suggesting that excessively short fragments compromise the initial R-loop nucleation despite cooperative binding.

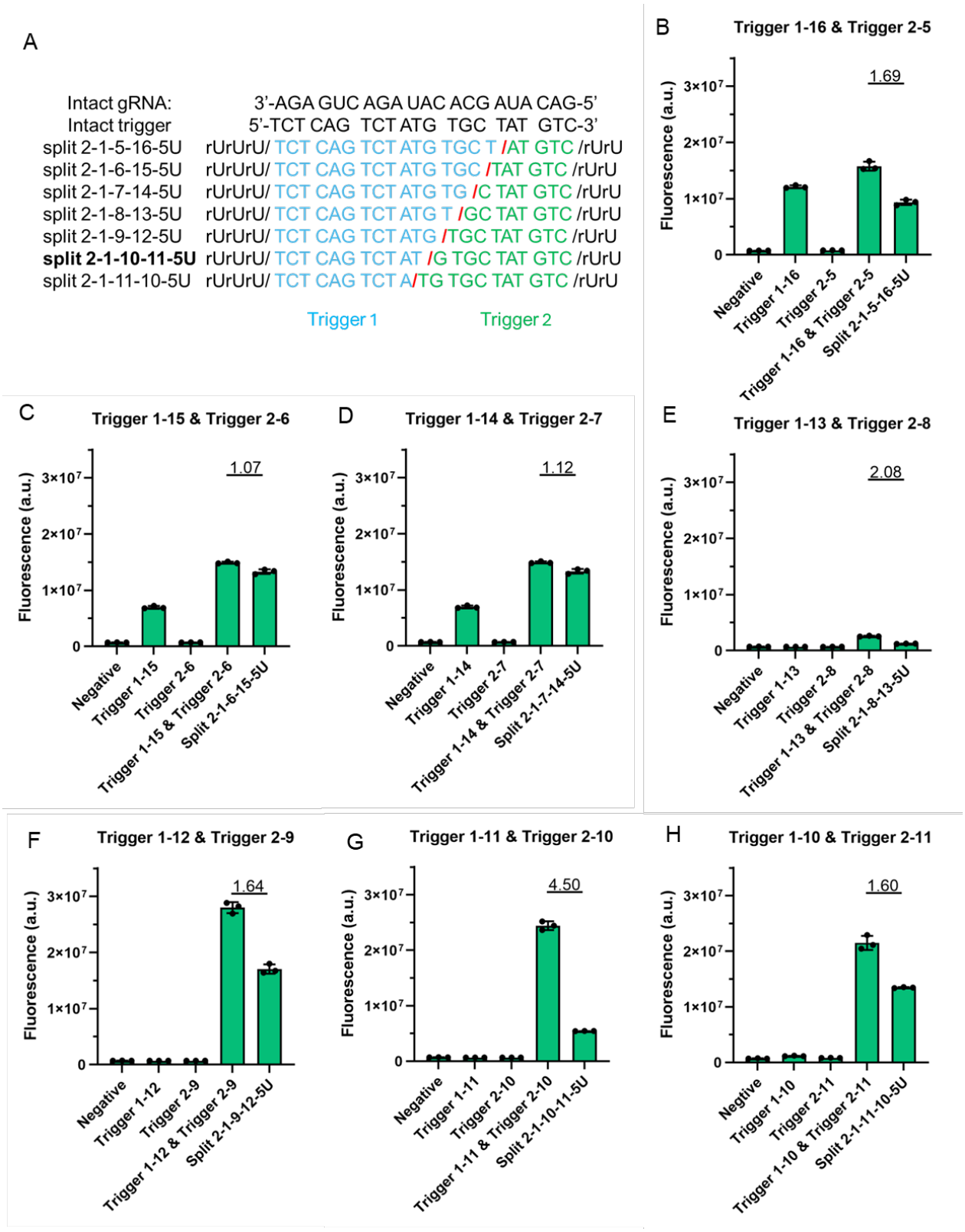
Collectively, these results define a clear length-dependent division of tasks between the split fragments: trigger-1 primarily governs the R-loop nucleation, while trigger-2 supports the R-loop extension and stabilization. An optimal window exists in which trigger-1 is sufficiently short to suppress background activation but long enough to initiate cooperative binding with trigger-2. The 11 nt + 10 nt split configuration best satisfies these constraints and was therefore selected as the optimal split-trigger design for subsequent STACS development.

bioRxiv preprint doi: https://doi.org/10.64898/2026.06.26.734747; this version posted August 4, 2026. The copyright holder for this preprint (which was not certified by peer review) is the author/funder, who has granted bioRxiv a license to display the preprint in perpetuity. It is made available under a CC-BY-NC-ND 4.0 International license.

A

Intact gRNA:	3'-AGA GUC AGA UAC ACG AUA CAG-5'
Intact trigger	5'-TCT CAG TCT ATG TGC TAT GTC-3'
split 2-1-5-16-5U	rUrUrU/ TCT CAG TCT ATG TGC T /AT GTC /rUrU
split 2-1-6-15-5U	rUrUrU/ TCT CAG TCT ATG TGC /TAT GTC /rUrU
split 2-1-7-14-5U	rUrUrU/ TCT CAG TCT ATG TG /C TAT GTC /rUrU
split 2-1-8-13-5U	rUrUrU/ TCT CAG TCT ATG T /GC TAT GTC /rUrU
split 2-1-9-12-5U	rUrUrU/ TCT CAG TCT ATG /TGC TAT GTC /rUrU
split 2-1-10-11-5U	rUrUrU/ TCT CAG TCT AT /G TGC TAT GTC /rUrU
split 2-1-11-10-5U	rUrUrU/ TCT CAG TCT A/TG TGC TAT GTC /rUrU

Trigger 1 Trigger 2



bioRxiv preprint doi: https://doi.org/10.64898/2026.06.26.734747; this version posted August 4, 2026. The copyright holder for this preprint (which was not certified by peer review) is the author/funder, who has granted bioRxiv a license to display the preprint in perpetuity. It is made available under a CC-BY-NC-ND 4.0 International license.

Figure 3. Defining the optimal length of trigger 1 and trigger 2. (A). Sequences of linear mediators with different lengths; (B-H). The ability of trigger 1 and trigger 2 with different lengths to activate LbCas12a. n=3, error bars represent mean ± SD, * $P \leqslant 0.05$, ** $P \leqslant 0.01$, *** $P \leqslant 0.001$, **** $P \leqslant 0.0001$, ns = non-significant, a.u = arbitrary units.

4. Performance evaluation of STACS

In STACS (Fig. 4A), target RNA is first recognized by sequence-programmed LbuCas13a, triggering robust collateral RNase activity. Each activated Cas13a RNP cleaves numerous linear DNA-RNA-DNA mediators, converting a single RNA recognition event into the generation of a large pool of physically independent split DNA fragments with external extensions. These cleavage products act as cooperative split triggers for LbCas12a, in which one fragment nucleates R-loop initiation while the complementary fragment promotes R-loop extension and stabilization, together activating otherwise inactive Cas12a RNPs. Consequently, numerous new Cas12a RNPs are activated downstream of a single target RNA molecule, transforming the conventional one-target one-Cas RNP paradigm into a cascade process with high Cas RNP activation multiplicity. The massively amplified Cas12a trans-cleavage activity then produces strong fluorescence or lateral-flow signals through reporter cleavage, enabling amplification-free, low-background, and ultrasensitive nucleic acid detection.

Based on this cascade architecture, the performance of STACS for SARS-CoV-2 RNA detection was evaluated using a multiple-gRNA recognition strategy (Fig. 4A). The *trans*-cleavage ability of LbuCas13a on linear mediator was demonstrated via both agarose gel electrophoresis analysis (Fig. S2) and fluorescent readout (Fig. S3) and the optimum buffer for STACS was found to be

bioRxiv preprint doi: https://doi.org/10.64898/2026.06.26.734747; this version posted August 4, 2026. The copyright holder for this preprint (which was not certified by peer review) is the author/funder, who has granted bioRxiv a license to display the preprint in perpetuity. It is made available under a CC-BY-NC-ND 4.0 International license.

rCutSmart (Fig. S4). Four LbuCas13a gRNAs targeting the N, M, E, and ORF regions of the viral genome were combined to enhance target engagement and maximize Cas13a activation, thereby increasing the probability of productive cascade initiation (Fig. S5). In addition, the incubation time of STACS was optimized to be close to 15min (Fig. S6).

Using this configuration, STACS enabled rapid and sensitive detection of reference SARS-CoV-2 RNA targets by using plate reader (Fig. S7). When 3.6 copies of reference SARS-CoV-2 Standards RNA were present per reaction, a clear and time-dependent fluorescence increase was observed compared with the negative control (Fig. 4B), confirming a successful cascade activation at near single-copy levels without enzymatic preamplification.

To demonstrate the relevance of STAC in a POCT setting, detection was performed using an LFA. We evaluated the detection range of STACS by testing reference SARS-CoV-2 standards across a wide RNA concentration range. As shown in Fig. 4C & 4D, STACS produced significantly elevated fluorescence signals for RNA inputs from 3.6 to 1006.1 copies per reaction compared with the negative control, indicating robust discrimination across more than two orders of magnitude. The consistent increase in signal with rising target concentration further supports the use of STACS for semi-quantitative analysis over this range.

Together, these results establish that STACS, when combined with a multiple-gRNA recognition strategy, enables rapid, amplification-free, and ultrasensitive detection of SARS-CoV-2 RNA with a broad dynamic range.

bioRxiv preprint doi: https://doi.org/10.64898/2026.06.26.734747; this version posted August 4, 2026. The copyright holder for this preprint (which was not certified by peer review) is the author/funder, who has granted bioRxiv a license to display the preprint in perpetuity. It is made available under a CC-BY-NC-ND 4.0 International license.

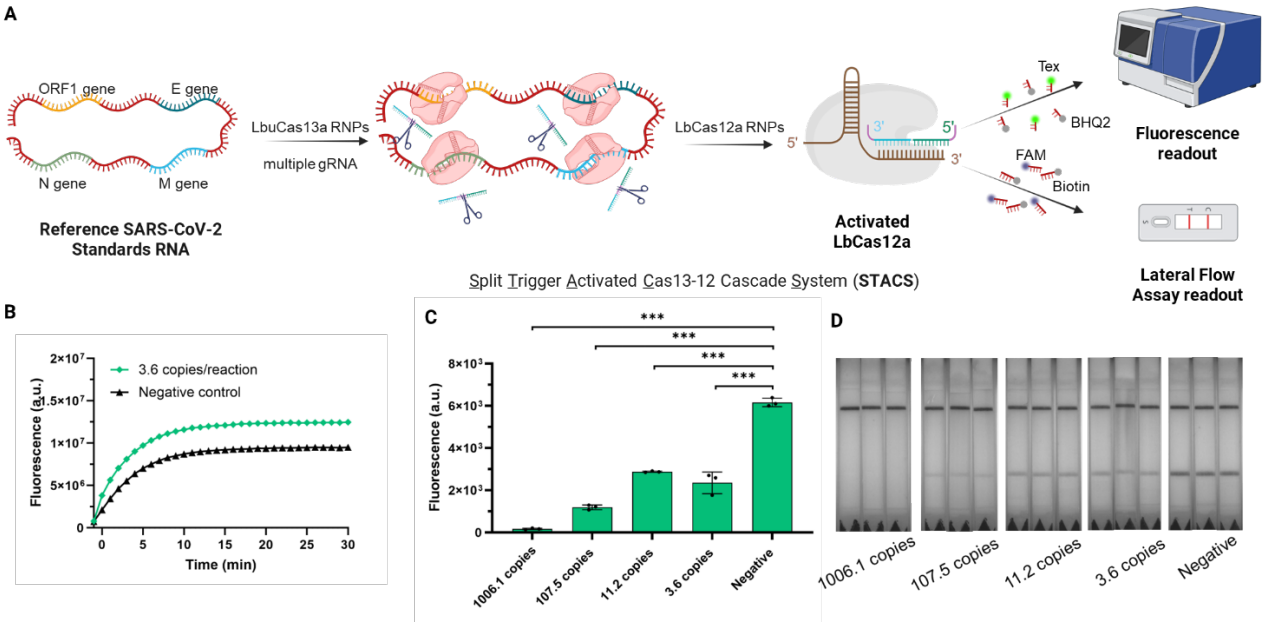


Figure 4. Performance evaluation of STACS using a multiple-gRNA strategy. (A) Schematic illustration of STACS employing four LbuCas13a gRNAs targeting the N, M, E, and ORF genes of reference SARS-CoV-2 Standards RNA. (B) Fluorescence kinetics of STACS for detection of 3.6 copies of reference SARS-CoV-2 Standards RNA. (C) The detection range of STACS for reference SARS-CoV-2 Standards RNA using LFA. (D). The corresponding images of figure C. n=3, error bars represent mean ± SD, * P ⩽ 0.05, ** P ⩽ 0.01, *** P ⩽ 0.001, **** P ⩽ 0.0001, ns = non-significant, a.u = arbitrary units.

5. The detection performance of STACS for SARS-CoV-2 in environmental samples

The applicability of STACS for SARS-CoV-2 RNA detection in complex environmental matrices was evaluated using mud samples as a representative challenge. The workflow for environmental sample processing is illustrated in Fig. 5A. Briefly, mud samples were filtered to remove potentially inhibitory particulates, and subsequently the synthetic SARS-CoV-2 genomic RNA

bioRxiv preprint doi: https://doi.org/10.64898/2026.06.26.734747; this version posted August 4, 2026. The copyright holder for this preprint (which was not certified by peer review) is the author/funder, who has granted bioRxiv a license to display the preprint in perpetuity. It is made available under a CC-BY-NC-ND 4.0 International license.

was tested by STACS. Before testing STACS, the activation ability of standard LbCas12a and LbuCas13a in 5% environmental mud sample was demonstrated (Fig. S8).

Using fluorescence-based readout, STACS enabled clear discrimination between positive and negative samples in mud matrices. As shown in Fig. 5B, reactions containing 100, 10, and 1 copies of synthetic SARS-CoV-2 genomic RNA produced significantly higher fluorescence signals compared with negative controls, demonstrating that STACS retains high analytical sensitivity in environmental samples despite matrix complexity.

Consistent results were obtained using LFA readout. Quantitative analysis of test line peak intensities revealed statistically significant differences between positive and negative samples across all tested concentrations (Fig. 5C). Representative LFA strips further confirmed that STACS could reliably detect as few as 1 copy of synthetic SARS-CoV-2 genomic RNA in filtered mud samples (Fig. 5D & Fig. S9).

Collectively, these results demonstrate that STACS maintains robust performance in environmentally relevant matrices following minimal sample preparation. The ability to sensitively detect low-copy viral RNA in mud highlights the potential of STACS for environmental surveillance applications, such as wastewater monitoring and field-based pathogen detection.

bioRxiv preprint doi: https://doi.org/10.64898/2026.06.26.734747; this version posted August 4, 2026. The copyright holder for this preprint (which was not certified by peer review) is the author/funder, who has granted bioRxiv a license to display the preprint in perpetuity. It is made available under a CC-BY-NC-ND 4.0 International license.

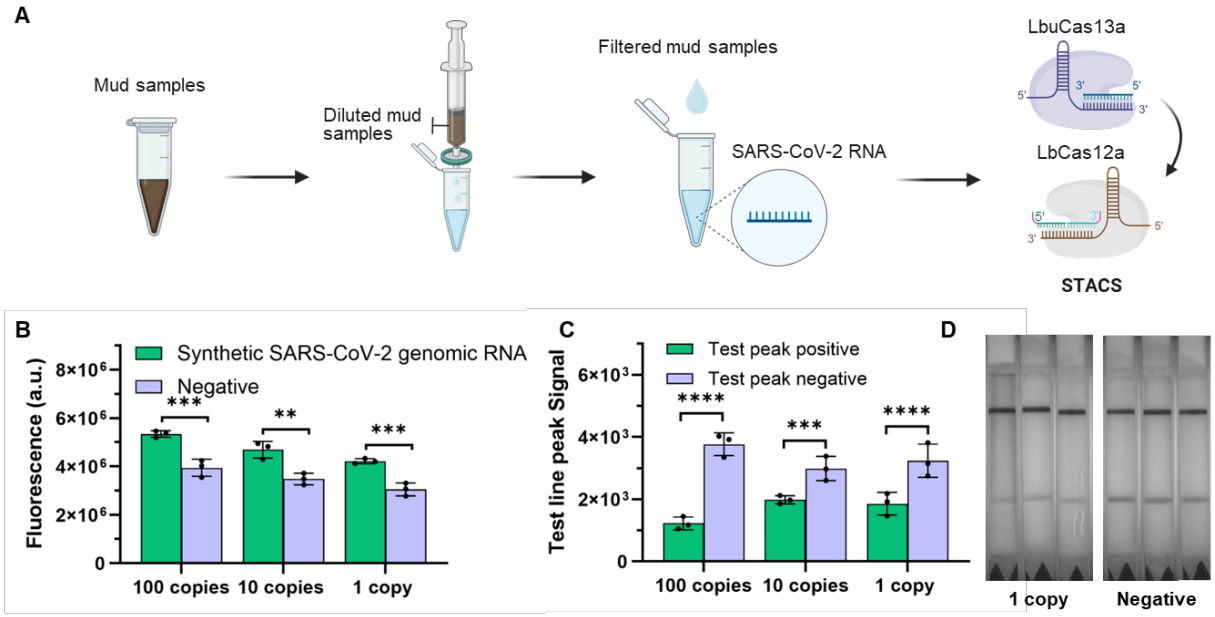


Figure 5. STACS application in environmental samples via fluorescent-based readout and LFA. (A). Schematic diagram of environmental mud sample preparation in STACS; (B) The detection ability of STACS for synthetic SARS-CoV-2 genomic RNA in 5% environmental mud sample via fluorescent-based readout; (C) The detection ability of STACS for synthetic SARS-CoV-2 genomic RNA in 5% environmental mud sample via LFA-based readout; (D) The corresponding LFA image of 1 copy in Figure C. n=3, error bars represent mean ± SD, * $P \leqslant 0.05$, ** $P \leqslant 0.01$, *** $P \leqslant 0.001$, **** $P \leqslant 0.0001$, ns = non-significant, a.u = arbitrary units.

6. Detection performance of STACS for SARS-CoV-2 in biological matrices

The performance of STACS in biological matrices was next evaluated using human serum as a representative sample. As illustrated in Fig. 6A, serum samples were pretreated with proteinase K followed by heat inactivation to mitigate matrix-associated interference prior to STACS

bioRxiv preprint doi: https://doi.org/10.64898/2026.06.26.734747; this version posted August 4, 2026. The copyright holder for this preprint (which was not certified by peer review) is the author/funder, who has granted bioRxiv a license to display the preprint in perpetuity. It is made available under a CC-BY-NC-ND 4.0 International license.

analysis. The pretreatment effect of proteinase K was demonstrated to be highly effective (Fig. S10).

Using fluorescence-based readout, STACS enabled reliable detection of synthetic SARS-CoV-2 genomic RNA in 10% human serum. As shown in Fig. 6B, samples containing 100, 10, and 1 copies of synthetic SARS-CoV-2 genomic RNA produced significantly higher fluorescence signals than negative controls, demonstrating that STACS retains high sensitivity in serum despite the presence of endogenous biomolecules.

Consistent results were obtained using LFA readout. Quantitative analysis of test line peak intensities revealed clear and statistically significant discrimination between positive and negative samples across all tested concentrations (Fig. 6C). Representative LFA strips further confirmed that STACS could detect as few as 1 copy of synthetic SARS-CoV-2 genomic RNA in serum samples following proteinase K pretreatment (Fig. 6D & Fig. S11). These results demonstrate that STACS maintains robust amplification-free detection performance in clinically relevant serum matrices after simple enzymatic pretreatment, supporting its potential utility for rapid molecular diagnostics in real biological samples.

bioRxiv preprint doi: https://doi.org/10.64898/2026.06.26.734747; this version posted August 4, 2026. The copyright holder for this preprint (which was not certified by peer review) is the author/funder, who has granted bioRxiv a license to display the preprint in perpetuity. It is made available under a CC-BY-NC-ND 4.0 International license.

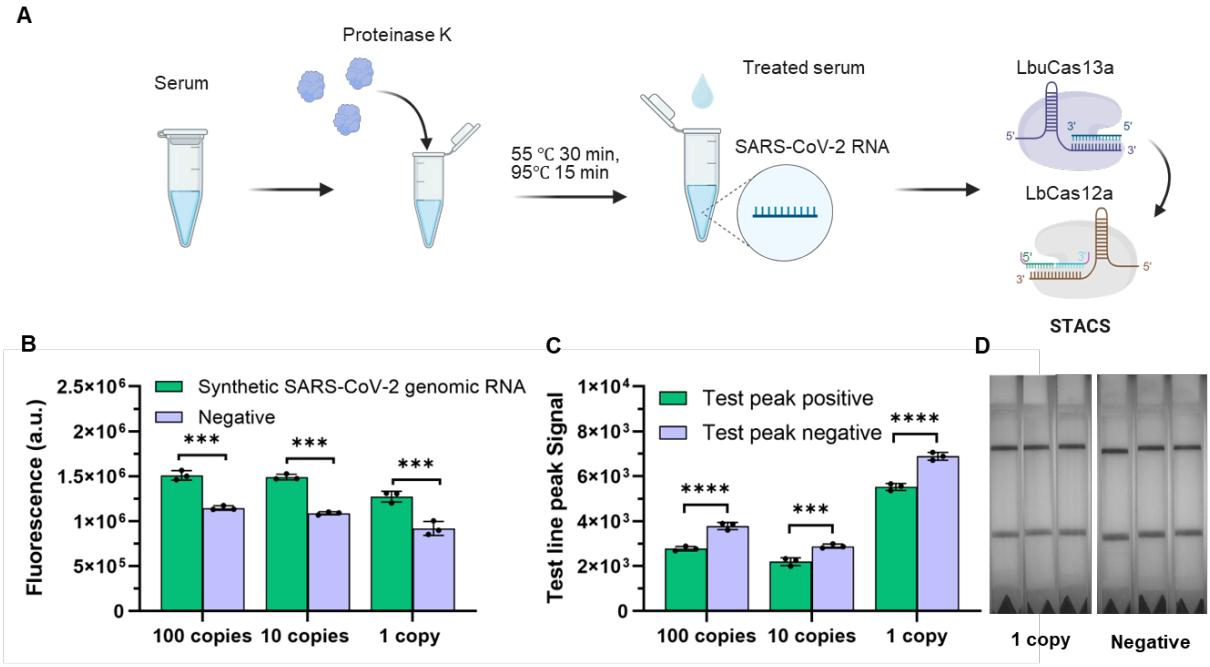


Figure 6. STACS application in 10% human serum via fluorescent-based readout and LFA. (A) Schematic diagram of human serum preparation in STACS; (B) The detection ability of STACS for 1-100 copies of synthetic SARS-CoV-2 genomic RNA in 10% human serum via fluorescent-based readout; (C) The detection ability of STACS for 1-100 copies of synthetic SARS-CoV-2 genomic RNA in 10% human serum via LFA readout (C); D. The corresponding images of 1 copy in Figure C. n=3, error bars represent mean ± SD, * P ⩽ 0.05, ** P ⩽ 0.01, *** P ⩽ 0.001, ns = non-significant.

Encouraged by the robust performance of STACS in serum and environmental matrices, we next evaluated its applicability in human saliva, a clinically relevant and non-invasive sample type (Fig. 7A). Saliva samples were processed by centrifugation to collect the supernatant, followed by proteinase K treatment and heat inactivation prior to STACS analysis. The activation abilities

bioRxiv preprint doi: https://doi.org/10.64898/2026.06.26.734747; this version posted August 4, 2026. The copyright holder for this preprint (which was not certified by peer review) is the author/funder, who has granted bioRxiv a license to display the preprint in perpetuity. It is made available under a CC-BY-NC-ND 4.0 International license.

of LbCas12a and LbuCas13a in proteinase K pretreated 10% human saliva were assessed and no significant reductions were observed (Fig. S12).

Using fluorescence-based readout, STACS enabled sensitive detection of reference SARS-CoV-2 Standards RNA spiked into 10% human saliva. As shown in Fig. 7B, samples containing 100.61, 42.5, 10.75, and 3.21 copies of reference SARS-CoV-2 RNA standards per reaction generated significantly higher fluorescence signals than negative controls, demonstrating reliable amplification-free detection down to low copy numbers in saliva.

We further assessed STACS performance across multiple individual saliva samples. When 12 independent human saliva samples were spiked with a final concentration of 3.21 copies of reference SARS-CoV-2 RNA standards, STACS consistently produced significantly higher fluorescence signals compared with corresponding negative controls (Fig. 7D), indicating good robustness against inter-individual sample variability.

To validate compatibility with point-of-care readout formats, the same saliva samples were analyzed using LFA. Quantitative analysis revealed a significant difference in test line peak signals between positive and negative samples at 3.21 copies (Fig. 7C), which was further supported by representative LFA images (Fig. 7E). These results demonstrate that STACS enables sensitive, amplification-free detection of SARS-CoV-2 RNA in human saliva following minimal sample processing, supporting its potential for non-invasive and point-of-care molecular diagnostics.

bioRxiv preprint doi: https://doi.org/10.64898/2026.06.26.734747; this version posted August 4, 2026. The copyright holder for this preprint (which was not certified by peer review) is the author/funder, who has granted bioRxiv a license to display the preprint in perpetuity. It is made available under a CC-BY-NC-ND 4.0 International license.

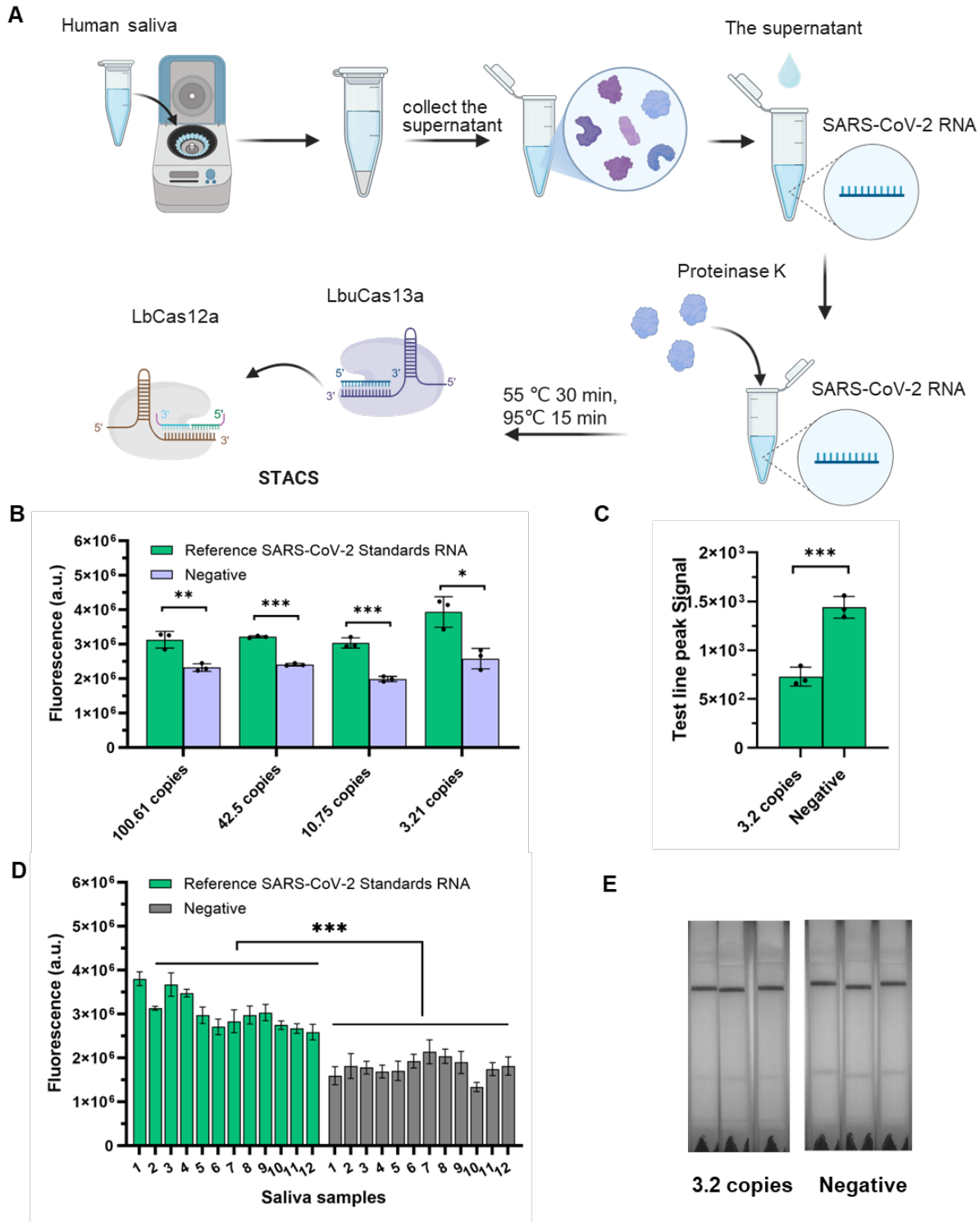


Figure 7. STACS application in 10% human saliva samples via fluorescent-based readout and LFA. (A) Schematic diagram of human serum preparation in STACS. (B) The detection range of

bioRxiv preprint doi: https://doi.org/10.64898/2026.06.26.734747; this version posted August 4, 2026. The copyright holder for this preprint (which was not certified by peer review) is the author/funder, who has granted bioRxiv a license to display the preprint in perpetuity. It is made available under a CC-BY-NC-ND 4.0 International license.

STACS for pretreatment saliva spiked in reference SARS-CoV-2 Standards RNA samples via fluorescence readout; (C). The detection of STACS for pretreatment saliva spiked in reference SARS-CoV-2 Standards RNA samples via LFA readout; (D). The detection of 3.2 copies of reference SARS-CoV-2 Standards RNA in 10% clinical human saliva samples (from 12 different people) after proteinase K pretreatment via fluorescent-based readout; (E). The detection of 3.2 copies of reference SARS-CoV-2 Standards RNA in 10% clinical human saliva (from 22 different people) after proteinase K pretreatment via LFA. n=3, error bars represent mean ± SD, * $P \leqslant 0.05$, ** $P \leqslant 0.01$, *** $P \leqslant 0.001$, ns = non-significant.

Discussion

In this study, we establish the molecular principles that define how fragmented nucleic acid triggers activate Cas12a and show how these principles collectively enable a cascade architecture that expands a single target recognition event into large-scale downstream Cas RNP activation. Our mechanistic analyses reveal three fundamental requirements for Cas12a activation by split triggers: (i) external nucleotide extensions are tolerated, whereas internal insertions disrupt spacer complementarity and abolish R-loop formation; (ii) activation strictly requires two physically independent fragments, as covalent linkage prevents the conformational flexibility needed for stepwise R-loop propagation; and (iii) efficient activation depends on precise fragment lengths, with a short seed-nucleating strand and a complementary R-loop extending strand providing the optimal synergistic configuration. These insights resolve the previously undefined sequence and structural rules governing split-trigger compatibility with Cas12a.

bioRxiv preprint doi: https://doi.org/10.64898/2026.06.26.734747; this version posted August 4, 2026. The copyright holder for this preprint (which was not certified by peer review) is the author/funder, who has granted bioRxiv a license to display the preprint in perpetuity. It is made available under a CC-BY-NC-ND 4.0 International license.

By mapping these mechanistic constraints, we demonstrate why LbuCas13a cleavage naturally produces mechanistically optimal activators - short, independent DNA fragments bearing external overhangs - which directly feed into Cas12a activation. Notably, the efficiency of LbuCas13a-mediated cleavage of the linear mediator represents a critical determinant of cascade performance, as it governs the rate and abundance of split-trigger generation required for downstream Cas12a activation. This coincidence enables a predictable, sequential signal relay in which Cas13-based RNA recognition is immediately converted into Cas12a-mediated DNA signal amplification without any enzymatic preamplification. The optimized split-trigger pair (11 nt + 10 nt) maximizes the R-loop seeding efficiency and underpins the high analytical sensitivity of the system.

Leveraging these design principles, we developed STACS, a linear mediator-powered Cas13-Cas12 tandem platform that achieves amplification-free detection down to 1 copy/μL within 15 minutes. Unlike conventional CRISPR assays(16-18), which rely on single-enzyme *trans*-cleavage, STACS decouples recognition and reporting into two orthogonal nucleases. This design enhances signal gain, suppresses background activation, and ensures that Cas12a activity occurs only when triggered by bona fide Cas13 cleavage products. As a result, STACS delivers PCR-level sensitivity without thermal cycling or isothermal amplification, substantially simplifying workflow and eliminating contamination risk.

Importantly, the robustness of the STACS linear mediators translates into strong performance across diverse sample matrices, including human serum, human saliva, and environmental mud. Proteinase K treatment effectively stabilizes split mediators in biological fluids, while simple filtration restores CRISPR activity in environmental samples. Across all matrices, STACS consistently detected SARS-CoV-2 genomic RNA at low copy numbers, demonstrating its utility

bioRxiv preprint doi: https://doi.org/10.64898/2026.06.26.734747; this version posted August 4, 2026. The copyright holder for this preprint (which was not certified by peer review) is the author/funder, who has granted bioRxiv a license to display the preprint in perpetuity. It is made available under a CC-BY-NC-ND 4.0 International license.

for point-of-care diagnostics, field surveillance, and rapid testing in resource-limited settings. Although this study employs certified SARS-CoV-2 reference materials with traceable quantification and demonstrates robust performance across complex biological and environmental matrices, the current results primarily establish analytical validity. Further work is required to achieve large-scale clinical validation, direct benchmarking against gold-standard methods such as RT-qPCR, and systematic evaluation of stability and deployment readiness. Future studies will focus on validating STACS using authentic clinical specimens to confirm its clinical applicability. In addition, while STACS exhibits concentration-dependent signal output, its cascade-driven nonlinear amplification positions it primarily as a highly sensitive qualitative detection platform with limited semi-quantitative capability.

More broadly, our mechanistic framework provides a foundation for rationally engineering CRISPR cascades (Table S1) (10,14,19-23). The rules uncovered here - extension position, fragment independence, and length-dependent R-loop dynamics - are generalizable and can inform the development of next-generation tandem architectures involving Cas12, Cas13, Cas14, and other emerging effectors. Because split-trigger activation enables modular signal gating and combinatorial logic(9), STACS also offers opportunities for multiplexed sensing, conditional activation circuits, and high-fidelity molecular computation.

Overall, this work bridges a critical mechanistic gap in Cas activation biology and demonstrates how fundamental insights into R-loop initiation and propagation can yield practical, high-performance diagnostic technologies. The linear mediator-powered Cas13-Cas12 cascade represents a versatile platform for rapid, ultralow-input, amplification-free RNA/DNA detection suitable for clinical diagnostics, non-invasive liquid biopsy, environmental pathogen monitoring, and next-generation point-of-care testing.

bioRxiv preprint doi: https://doi.org/10.64898/2026.06.26.734747; this version posted August 4, 2026. The copyright holder for this preprint (which was not certified by peer review) is the author/funder, who has granted bioRxiv a license to display the preprint in perpetuity. It is made available under a CC-BY-NC-ND 4.0 International license.

Conclusion

In this work, we define the molecular rules that govern Cas12a activation by fragmented nucleic acids and demonstrate how these principles can be exploited to engineer a programmable Cas13-Cas12 tandem detection system. We reveal that Cas12a activation depends critically on extension position, fragment independence, and optimized trigger length - mechanistic constraints that together determine whether split activators can successfully nucleate and propagate the R-loop. These insights explain why Cas13-mediated cleavage naturally produces functional Cas12a activators and provide a rational framework for designing future CRISPR sensing cascades.

Building on these mechanistic foundations, we developed STACS, an amplification-free Cas13-Cas12 cascade capable of detecting RNA targets at 1 copy/μL within 15 minutes. The platform maintains high analytical sensitivity across clinically and environmentally relevant matrices, including serum, saliva, and mud, and is compatible with both fluorescence and lateral-flow readouts. By decoupling RNA recognition from DNA reporting through a linear DNA-RNA-DNA mediator, STACS integrates mechanistic precision with practical robustness, enabling ultrafast and field-deployable molecular diagnostics. This study bridges a key mechanistic gap in CRISPR activation biology and introduces a versatile cascade architecture that supports rapid, low-input RNA/DNA detection for point-of-care testing, environmental surveillance, and translational biomedical applications.

Acknowledgements

The authors acknowledge the support of the Australia's Economic Accelerator (AEA) (AE240300106) of FD. and the ARC Discovery funding (DP240103024) to EMG and FD. The authors thank Ms Avin Mohammadnejad Mavaneh for her technical assistance in AEA project.

bioRxiv preprint doi: https://doi.org/10.64898/2026.06.26.734747; this version posted August 4, 2026. The copyright holder for this preprint (which was not certified by peer review) is the author/funder, who has granted bioRxiv a license to display the preprint in perpetuity. It is made available under a CC-BY-NC-ND 4.0 International license.

Author contributions

Methodology: R.S., F.D.; validation: R.S., F.D.; formal analysis: R.S., F.D.; writing-original draft: R.S., F.D.; writing-review: F.D., E.G.; supervision, funding acquisition, and project administration: F.D., E.G.

Declaration of interests

The authors declare no competing interests.

Materials and Methods

All nucleic acid sequences listed in Table 1 were purchased from Gencefe Biotechnology Co. Ltd (Jiangsu, China). LbuCas13a protein (Z03742-1) was purchased from GenScript Biotech (Nanjing, China). LbCas12a protein (M0653T) and rCutSmart buffer (B6004S) were purchased from NEB Biotechnology Co. (Ipswich, MA UK). DNase/RNase Free Water (10977015), Proteinase K (25530049) were purchased from Thermo Fisher Scientific (Waltham, MA US). Human serum (H4522) was purchased from Sigma-Aldrich (St. Louis, Missouri US). Milenia HybriDetect LFA kit (MGHD 1) was purchased from Milenia Biotec Gmbh (Giessen, Germany). SARS-CoV-2 Standards (NMIA NA050-NA055, B200921) were provided by Australian Government National Measurement Institute.

Table 1. DNA and RNA oligos are utilized in this study.

Name	Oligo type	Sequence 5'-3'	Modification
Intact trigger	ssDNA	TCT CAG TCT ATG TGC TAT GTC	N/A
split 1-2-1U	RNA-DNA	TCT CAG TCT A/rU/ TG TGC TAT GTC	N/A
split 1-2-3U	RNA-DNA	TCT CAG TCT A/rUrUrU/ TG TGC TAT GTC	N/A

bioRxiv preprint doi: https://doi.org/10.64898/2026.06.26.734747; this version posted August 4, 2026. The copyright holder for this preprint (which was not certified by peer review) is the author/funder, who has granted bioRxiv a license to display the preprint in perpetuity. It is made available under a CC-BY-NC-ND 4.0 International license.

split 1-2-5U	RNA-DNA	TCT CAG TCT A/rUrUrUrUrU/ TG TGC TAT GTC	N/A
split 1-2-7U	RNA-DNA	TCT CAG TCT A/rUrUrUrUrUrUrU/ TG TGC TAT GTC	N/A
split 1-2-5U-F	RNA-DNA	TCT CAG TCT A/rUrUrUrUrU/ TG TGC TAT GTC	5'- Texas Red; 3'-BHQ2
split 2-1-10-11-5U-F	RNA-DNA	G TGC TAT GTC /rUrUrUrUrU/ TCT CAG TCT AT	5'- Texas Red; 3' -BHQ2
split 2-1-1U	RNA-DNA	TG TGC TAT GTC /rU/ TCT CAG TCT A	N/A
split 2-1-3U	RNA-DNA	TG TGC TAT GTC /rUrUrU/ TCT CAG TCT A	N/A
split 2-1-5U	RNA-DNA	TG TGC TAT GTC /rUrUrUrUrU/ TCT CAG TCT A	N/A
trigger-1-3U-3'	RNA-DNA	TCT CAG TCT A/rUrUrU/	N/A
trigger-2-3U-5'	RNA-DNA	/rUrUrU/ TG TGC TAT GTC	N/A
trigger-1-3U-5'	RNA-DNA	/rUrUrU/ TCT CAG TCT A	N/A
trigger-2-3U-3'	RNA-DNA	TG TGC TAT GTC /rUrUrU/	N/A
trigger-1-10	DNA	TCT CAG TCT A	N/A
trigger-2-11	DNA	TG TGC TAT GTC	N/A
trigger-1-13	DNA	TCT CAG TCT ATG T	N/A
trigger-2-8	DNA	GC TAT GTC	N/A
split 2-1-8-13-5U	RNA-DNA	GC TAT GTC /rUrUrUrUrU/ TCT CAG TCT ATG T	N/A
trigger-1-16	DNA	TCT CAG TCT ATG TGC T	N/A
trigger-2-5	DNA	AT GTC	N/A
split 2-1-5-16-5U	RNA-DNA	AT GTC /rUrUrUrUrU/ TCT CAG TCT ATG TGC T	N/A
trigger-1-12	DNA	TCT CAG TCT ATG	N/A
trigger-2-9	DNA	TGC TAT GTC	N/A
split 2-1-9-12-5U	RNA-DNA	TGC TAT GTC /rUrUrUrUrU/ TCT CAG TCT ATG	N/A
trigger-1-11	DNA	TCT CAG TCT AT	N/A
trigger-2-10	DNA	G TGC TAT GTC	N/A

bioRxiv preprint doi: https://doi.org/10.64898/2026.06.26.734747; this version posted August 4, 2026. The copyright holder for this preprint (which was not certified by peer review) is the author/funder, who has granted bioRxiv a license to display the preprint in perpetuity. It is made available under a CC-BY-NC-ND 4.0 International license.

split 2-1-10-11-5U	RNA-DNA	G TGC TAT GTC /rUrUrUrUrU/ TCT CAG TCT AT	N/A
trigger-1-14	DNA	TCT CAG TCT ATG TG	N/A
trigger-2-7	DNA	C TAT GTC	N/A
split 2-1-7-14-5U	RNA-DNA	C TAT GTC /rUrUrUrUrU/ TCT CAG TCT ATG TG	N/A
trigger-1-15	DNA	TCT CAG TCT ATG TGC	N/A
trigger-2-6	DNA	TAT GTC	N/A
split 2-1-6-15-5U	RNA-DNA	TAT GTC /rUrUrUrUrU/ TCT CAG TCT ATG TGC	N/A
N gene	RNA	GGG GCG CGA UCA AAA CAA CG	N/A
M gene	RNA	ACG AAC GCU UUC UUA UUA CA	N/A
E gene	RNA	UAU UGU UAA CGU GAG UCU UG	N/A
ORF gene	RNA	GAU GAG UGG AGU AUG GCU AC	N/A
Intact gRNA	ssRNA	UAA UUU CUA CUA AGU GUA GAU GAC AUA GCA CAU AGA CUG AGA	N/A
N-gene gRNA	ssRNA	GGA CCA CCC CAA AAA CGA AGG GGA CUA AAA CAC GUU GUU UUG AUC GCG CCC C	N/A
M-gene gRNA	ssRNA	GGA CCA CCC CAA AAA CGA AGG GGA CUA AAA CAU GUA AUA AGA AAG CGU UCG U	N/A
E-gene gRNA	ssRNA	GGA CCA CCC CAA AAA CGA AGG GGA CUA AAA CAC AAG ACU CAC GUU AAC AAU A	N/A
ORF-gene gRNA	ssRNA	GGA CCA CCC CAA AAA CGA AGG GGA CUA AAA CAG UAG CCA UAC UCC ACU CAU C	N/A

Preparation of the standard CRISPR reaction solution

The standard CRISPR reaction solution of LbCas12a and LbuCas13a were prepared as follows:

LbCas12a: 1 μL of 20 μM of LbCas12a endonuclease and 1 μL of 20 μM of Intact trigger gRNA were mixed at 1 mL 1× rCutSmart buffer, followed by addition of 5 μL of 100 μM of 6C reporter. The prepared standard CRISPR/Cas12a reaction mixture was preincubated for 30 min at 37℃ and then stored at 4℃ for future use.

bioRxiv preprint doi: https://doi.org/10.64898/2026.06.26.734747; this version posted August 4, 2026. The copyright holder for this preprint (which was not certified by peer review) is the author/funder, who has granted bioRxiv a license to display the preprint in perpetuity. It is made available under a CC-BY-NC-ND 4.0 International license.

LbuCas13a: 1 µL of 20 µM of LbuCas13a endonuclease and 1 µL of 20 µM of LbuCas13a SARS-CoV-2 gRNA were mixed at 1 mL 1× rCutSmart buffer, followed by addition of 5 µL of 100 µM of split mediator or 5U reporter. The prepared standard CRISPR/Cas13a reaction mixture was preincubated for 30 min at 37℃ and then stored at 4℃ for future use.

Investigation of trigger mechanism of split mediator for Lbcas12a RNP

To investigate different split mediators' activation mechanism for Lbcas12a, 2µL of 1µM of trigger (split 1, split 2, split 1 & split 2 and split mediators) was added into 98 µL of standard CRISPR/ LbCas12a reaction solution (20nM of LbCas12a protein, 20nM of gRNA, 500nM of reporter, and 1mL of rCutSmart buffer). The reaction was carried out at 37 ℃, and the fluorescence intensity at Ex/Em of 570/615 nm was determined by using a plate reader (iD5 Spectramax, Molecular Devices, USA).

Multiple gRNA reaction buffer:

The CRISPR reaction solution of LbCas12a and LbuCas13a for multiple gRNA reaction were prepared as follows:

LbuCas13a: 4 µL of 20 µM of LbuCas13a endonuclease and 4 µL of 20 µM of LbuCas13a SARS-CoV-2 gRNA (specific to N gene, M gene, E gene or ORF gene) were mixed at 1 mL 1× rCutSmart buffer, followed by preincubation for 30 min at 37℃. Then, these four different RNP solutions were mixed and 6 µL of 10 µM of split mediator were added and stored at 4℃ for future use.

10×LbCas12a: 40 µL of 20 µM of LbCas12a endonuclease and 40 µL of 20 µM of Intact trigger gRNA were mixed at 1 mL 1× rCutSmart buffer, followed by addition of 1.66 µL of 100 µM of

bioRxiv preprint doi: https://doi.org/10.64898/2026.06.26.734747; this version posted August 4, 2026. The copyright holder for this preprint (which was not certified by peer review) is the author/funder, who has granted bioRxiv a license to display the preprint in perpetuity. It is made available under a CC-BY-NC-ND 4.0 International license.

6C/8C reporter. The prepared standard CRISPR/Cas12a reaction mixture was preincubated for 30 min at 37℃ and then stored at 4℃ for future use.

Detection of synthetic SARS-CoV-2 genomic RNA

To investigate the LOD of STACS for synthetic SARS-CoV-2 genomic RNA detection, 10 μL of 10,000 copies/mL, 1,000 copies/mL, 100 copies/mL of synthetic SARS-CoV-2 genomic RNA was added into 90 μL of standard multiple gRNA CRISPR/ LbuCas13a reaction solution for activating *trans*-cleavage of LbuCas13a. The reaction mixture was incubated at 37 ℃ for 30 min, followed by adding 10 μL of 10 times standard multiple gRNA CRISPR/ LbCas12a reaction solution. The fluorescence intensity at Ex/Em of 570/615 nm was determined by using a plate reader (iD5 Spectramax, Molecular Devices, USA) at 37 ℃.

Detection of synthetic SARS-CoV-2 genomic RNA in human serum

Proteinase K treatment: 40 μL of human serum were mixed with 20 μL of proteinase K (20mg/ml). The reaction solutions were incubated at 55 ℃ for 30 min and then 95 ℃ for 15 min, followed by cooling down to room temperature.

To investigate the detection ability of STACS for synthetic SARS-CoV-2 genomic RNA in 10% human serum, 10 μL of 10,000 copies/mL, 1,000 copies/mL, 100 copies/mL of synthetic SARS-CoV-2 genomic RNA in DPBS with 10% human serum was added into 90 μL of standard multiple gRNA-CRISPR/LbuCas13a reaction solution for activating *trans*-cleavage of LbuCas13a. The reaction mixture was incubated at 37 ℃ for 30 min, followed by adding 10 μL of 10 times standard multiple gRNA-CRISPR/LbCas12a reaction solution. The fluorescence intensity at Ex/Em of 570/615 nm was determined by using a plate reader (iD5 Spectramax, Molecular Devices, USA) at 37 ℃.

bioRxiv preprint doi: https://doi.org/10.64898/2026.06.26.734747; this version posted August 4, 2026. The copyright holder for this preprint (which was not certified by peer review) is the author/funder, who has granted bioRxiv a license to display the preprint in perpetuity. It is made available under a CC-BY-NC-ND 4.0 International license.

All human serum experiments were approved by the UNSW Ethics Committee (UNSW HC210160).

Detection of synthetic SARS-CoV-2 genomic RNA in environmental samples

Sample preparation was carried out as follows. Environmental mud samples were diluted 10 times in water and then filtered by 0.22 μm syringe filter and stored at 4 ℃ until further use.

To investigate the detection ability of STACS for synthetic SARS-CoV-2 genomic RNA in environmental samples, 10 μL of 10,000 copies/mL, 1,000 copies/mL, 100 copies/mL of synthetic SARS-CoV-2 genomic RNA in 1 × rCutSmart with 5% mud was added into 90 μL of standard multiple gRNA-CRISPR/LbuCas13a reaction solution for activating *trans*-cleavage of LbuCas13a. The reaction mixture was incubated at 37 ℃ for 30 min, followed by adding 10 μL of 10 times standard multiple gRNA-CRISPR/LbCas12a reaction solution. The fluorescence intensity at Ex/Em of 570/615 nm was determined by using a plate reader (iD5 Spectramax, Molecular Devices, USA) at 37 ℃.

Detection of SARS-CoV-2 Standards RNA

To investigate the detection ability of STACS for reference SARS-CoV-2 Standards RNA, 10 μL of 100,610 copies/mL, 10,750 copies/mL, 1,120 copies/mL or 360 copies/mL of reference SARS-CoV-2 Standards RNA was added into 90 μL of standard multiple gRNA CRISPR/LbuCas13a reaction solution. The reaction mixture was incubated at 37 ℃ for 30 min, followed by adding 10 μL of 10 times standard multiple gRNA-CRISPR/LbCas12a reaction solution. The fluorescence intensity at Ex/Em of 570/615 nm was determined by using a plate reader (iD5 Spectramax, Molecular Devices, USA) at 37 ℃.

Detection of reference SARS-CoV-2 Standards RNA in human saliva

bioRxiv preprint doi: https://doi.org/10.64898/2026.06.26.734747; this version posted August 4, 2026. The copyright holder for this preprint (which was not certified by peer review) is the author/funder, who has granted bioRxiv a license to display the preprint in perpetuity. It is made available under a CC-BY-NC-ND 4.0 International license.

Proteinase K treatment was carried out as follows. Briefly, 4 µL of proteinase K (20 mg/mL) was mixed with 32 µL of undiluted human saliva and 4 µL of reference SARS-CoV-2 Standards RNA (100,610 copies/mL; 42,500 copies/mL; 10,750 copies/mL; 3,210 copies/mL) or DPBS (as negative control). The mixture was incubated at 65 ℃ for 15 min and 95 ℃ for 5 min, followed by cooling down to 4 ℃ until further use.

To investigate the detection ability of STACS for reference SARS-CoV-2 Standards RNA in human saliva samples, 10 µL of 10,061 copies/mL, 4,250 copies/mL, 1,075 copies/mL, 321 copies/mL of reference SARS-CoV-2 Standards RNA in human saliva was added into 90 µL of standard multiple gRNA CRISPR/ LbuCas13a reaction solution. The reaction mixture was incubated at 37 ℃ for 30 min, followed by adding 10 µL of 10 times standard multiple gRNA-CRISPR/ LbCas12a reaction solution. The fluorescence intensity at Ex/Em of 570/615 nm was determined by using a plate reader (iD5 Spectramax, Molecular Devices, USA) at 37 ℃.

All human saliva experiments were approved by the UNSW Ethics Committee (UNSW HC 200568).

Lateral flow assays (LFA)

To investigate the detection ability of STACS for SARS-CoV-2 Standards RNA via LFA, 10 µL of synthetic SARS-CoV-2 genomic RNA or reference SARS-CoV-2 Standards RNA was added into 90 µL of standard multiple gRNA-CRISPR/LbuCas13a reaction solution for activating *trans*-cleavage of LbuCas13a. The reaction mixture was incubated at 37 ℃ for 30 min, followed by adding 10 µL of 10 times standard multiple gRNA-CRISPR/ LbCas12a reaction solution (using 8C as reporter). Then, 6 µL of reaction solution were mixed with 94 µL of Milenia running buffer at 2 min, 5 min, 7 min, 15 min, 30 min, followed by adding Milenia HybriDetect

bioRxiv preprint doi: https://doi.org/10.64898/2026.06.26.734747; this version posted August 4, 2026. The copyright holder for this preprint (which was not certified by peer review) is the author/funder, who has granted bioRxiv a license to display the preprint in perpetuity. It is made available under a CC-BY-NC-ND 4.0 International license.

1 strip into the tube and allowed to run for around 3 minutes. Lastly, strips were read on a lateral Flow Reader (AX-2X-S, Axxin Pty Ltd, Australia).

Reference

1. Feng, W., Peng, H., Zhang, H., Weinfeld, M. and Le, X.C. (2024) A Sensitive Technique Unravels the Kinetics of Activation and Trans-Cleavage of CRISPR-Cas Systems. *Angewandte Chemie*, **136**, e202404069.
2. Gootenberg, J.S., Abudayyeh, O.O., Lee, J.W., Essletzbichler, P., Dy, A.J., Joung, J., Verdine, V., Donghia, N., Daringer, N.M. and Freije, C.A. (2017) Nucleic acid detection with CRISPR-Cas13a/C2c2. *Science*, **356**, 438-442.
3. Chen, J.S., Ma, E., Harrington, L.B., Da Costa, M., Tian, X., Palefsky, J.M. and Doudna, J.A. (2018) CRISPR-Cas12a target binding unleashes indiscriminate single-stranded DNase activity. *Science*, **360**, 436-439.
4. Harrington, L.B., Burstein, D., Chen, J.S., Paez-Espino, D., Ma, E., Witte, I.P., Cofsky, J.C., Kyrpides, N.C., Banfield, J.F. and Doudna, J.A. (2018) Programmed DNA destruction by miniature CRISPR-Cas14 enzymes. *Science*, **362**, 839-842.
5. Kaminski, M.M., Abudayyeh, O.O., Gootenberg, J.S., Zhang, F. and Collins, J.J. (2021) CRISPR-based diagnostics. *Nature biomedical engineering*, **5**, 643-656.
6. Nalefski, E.A., Kooistra, R.M., Parikh, I., Hedley, S., Rajaraman, K. and Madan, D. (2024) Determinants of CRISPR Cas12a nuclease activation by DNA and RNA targets. *Nucleic Acids Research*, **52**, 4502-4522.
7. Fei, X., Lei, C., Ren, W., Liu, X. and Liu, C. (2023) Regulating the trans-cleavage activity of CRISPR/Cas12a by using an elongation-caged single-stranded DNA activator and the biosensing applications. *Analytical Chemistry*, **95**, 12169-12176.
8. Ma, J.-Y., Wang, S.-Y., Du, Y.-C., Wang, D.-X., Tang, A.-N., Wang, J. and Kong, D.-M. (2022) "RESET" effect: random extending sequences enhance the trans-cleavage activity of CRISPR/Cas12a. *Analytical Chemistry*, **94**, 8050-8057.
9. He, W., Li, X., Li, X., Guo, M., Zhang, M., Hu, R., Li, M., Ding, S. and Yan, Y. (2024) Split activator of CRISPR/Cas12a for direct and sensitive detection of microRNA. *Analytica Chimica Acta*, **1303**, 342477.
10. Deng, F., Li, Y., Yang, B., Sang, R., Deng, W., Kansara, M., Lin, F., Thavaneswaran, S., Thomas, D.M. and Goldys, E.M. (2024) Topological barrier to Cas12a activation by circular DNA nanostructures facilitates autocatalysis and transforms DNA/RNA sensing. *Nature Communications*, **15**, 1818.
11. Zhu, Z., Li, X., Ding, L. and Wu, T. (2025) Exploring the effect of activator topology on CRISPR–Cas12a trans-cleavage activity. *Nucleic Acids Research*, **53**, gkaf311.
12. Rananaware, S., Vesco, E., Shoemaker, G., Anekar, S., Sandoval, L., Meister, K., Macaluso, N., Nguyen, L. and Jain, P. (2023).

bioRxiv preprint doi: https://doi.org/10.64898/2026.06.26.734747; this version posted August 4, 2026. The copyright holder for this preprint (which was not certified by peer review) is the author/funder, who has granted bioRxiv a license to display the preprint in perpetuity. It is made available under a CC-BY-NC-ND 4.0 International license.

13. Li, Q., Song, Z.-L., Zhang, Y., Zhu, L., Yang, Q., Liu, X., Sun, X., Chen, X., Kong, R. and Fan, G.-C. (2023) Synergistic incorporation of two ssDNA activators enhances the trans-cleavage of CRISPR/Cas12a. *Analytical Chemistry*, **95**, 8879-8888.
14. Sun, K., Pu, L., Chen, C., Chen, M., Li, K., Li, X., Li, H. and Geng, J. (2024) An autocatalytic CRISPR-Cas amplification effect propelled by the LNA-modified split activators for DNA sensing. *Nucleic Acids Research*, **52**, e39-e39.
15. Li, S.-Y., Cheng, Q.-X., Wang, J.-M., Li, X.-Y., Zhang, Z.-L., Gao, S., Cao, R.-B., Zhao, G.-P. and Wang, J. (2018) CRISPR-Cas12a-assisted nucleic acid detection. *Cell discovery*, **4**, 20.
16. Deng, F., Li, Y., Li, B. and Goldys, E.M. (2022) Increasing trans-cleavage catalytic efficiency of Cas12a and Cas13a with chemical enhancers: Application to amplified nucleic acid detection. *Sensors and Actuators B: Chemical*, **373**, 132767.
17. Li, Y., Deng, F., Hall, T., Vesey, G. and Goldys, E.M. (2021) CRISPR/Cas12a-powered immunosensor suitable for ultra-sensitive whole Cryptosporidium oocyst detection from water samples using a plate reader. *Water research*, **203**, 117553.
18. Li, Y., Deng, F. and Goldys, E.M. (2022) A simple and versatile CRISPR/Cas12a-based immunosensing platform: Towards attomolar level sensitivity for small protein diagnostics. *Talanta*, **246**, 123469.
19. Sha, Y., Huang, R., Huang, M., Yue, H., Shan, Y., Hu, J. and Xing, D. (2021) Cascade CRISPR/cas enables amplification-free microRNA sensing with fM-sensitivity and single-base-specificity. *Chemical Communications*, **57**, 247-250.
20. Zhang, Y., Chen, Y., Zhang, Q., Liu, Y. and Zhang, X. (2023) An aM-level sensitive cascade CRISPR-Dx system (ASCas) for rapid detection of RNA without pre-amplification. *Biosensors and Bioelectronics*, **230**, 115248.
21. Deng, F., Sang, R., Li, Y., Yang, B., Zhai, X., Xue, R., Zhang, C., Deng, W. and Goldys, E.M. (2025) Hairpin-locker mediated CRISPR/Cas tandem system for ultrasensitive detection of DNA without pre-amplification. *Microchemical Journal*, **210**, 113025.
22. Shi, K., Xie, S., Tian, R., Wang, S., Lu, Q., Gao, D., Lei, C., Zhu, H. and Nie, Z. (2021) A CRISPR-Cas autocatalysis-driven feedback amplification network for supersensitive DNA diagnostics. *Science Advances*, **7**, eabc7802.
23. Zhou, Z., Lau, C.-H., Wang, J., Guo, R., Tong, S., Li, J., Dong, W., Huang, Z., Wang, T. and Huang, X. (2024) Rapid and amplification-free nucleic acid detection with DNA substrate-mediated autocatalysis of CRISPR/Cas12a. *ACS omega*, **9**, 28866-28878.